JOC Featured Article

Kinetic Studies on the Stability and Reactivity of β-Amino Alkylzinc Iodides Derived from Amino Acids

Ian Rilatt and Richard F. W. Jackson*

Department of Chemistry, The University of Sheffield, Dainton Building, Sheffield S3 7HF, United Kingdom

r.f.w.jackson@shef.ac.uk

Received August 7, 2008

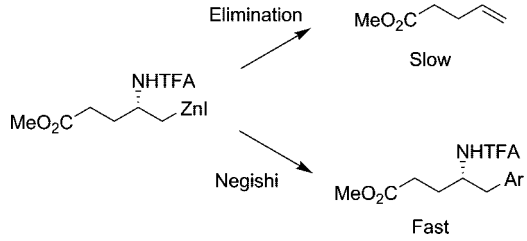

β-Amino alkylzinc iodides are intrinsically unstable toward β-elimination and protonation. The aim of this study was to determine the rates of these processes and also to understand how the reactivity of a range of β-amino alkylzinc iodides in Negishi cross-coupling reactions is influenced by the presence of functional groups within the zinc reagent. Decomposition of β-benzamido alkylzinc iodides occurs by protonation, and the first-order rate constant for the self-protonation of the carbon−zinc bond in reagent **4b** was determined to be 5.2×10^{-6} s^{-1} (at 291 K). In contrast, the carbamate derivative **2** decomposes by a first-order elimination process. The homologous reagent **3**, derived from glutamic acid, decomposes more quickly by β-elimination, with a first-order rate constant of 24×10^{-6} s^{-1} (at 291 K). Reagents **23** and **25**, in which the Boc group has been replaced with a trifluoroacetyl group, are more stable toward β-elimination than the corresponding reagents **2** and **3**, a striking outcome given that the trifluoroacetamido group is a better leaving group. Moreover, this replacement also changes the mechanism of the elimination to a second order process. Pseudo-second-order rate constants for the Negishi cross-coupling of reagents **2**, **3**, **23**, and **25** with iodobenzene have been determined, revealing the higher reactivity of the glutamic acid-derived reagents **3** and **25**. The main factor influencing reactivity, therefore, is determined to be the proximity of the ester group, rather than the nature of the nitrogen protecting group. Finally, β-amino alkylzinc iodides **46**−**48** containing Weinreb amides have been prepared, rate constants for their decomposition through elimination determined, and their synthetic potential for the preparation of β-amino ketones established.

Introduction

β-Amino alkylzinc iodides, derived from enantiomerically pure amino acids, have proven to be valuable synthetic intermediates, since they react using Pd or Cu catalysis with a wide range of electrophiles.[1] Reagent **1**, derived from serine,[2,3] has been widely employed in the synthesis of α-amino acids, while reagents **2** and **3**, derived from aspartic and glutamic acids, respectively, have been developed for the preparation of β- and γ-amino acids.[4] These reagents all give higher yields when prepared in dipolar aprotic solvents, the most convenient being DMF. However, each of these β-amino alkylzinc iodides is intrinsically unstable toward β-elimination, forming the corresponding alkene. In addition, such functionalized alkylzinc iodides can, in principle, decompose either by reaction with external proton donors or through self-protonation. All these side-reactions can reduce the yield in desired carbon−carbon bond-forming reactions. The aim of this study has been to quantify these effects and also to understand how the reactivity of a range of β-amino alkylzinc iodides in Negishi cross-

(1) Rilatt, I.; Caggiano, L.; Jackson, R. F. W. *Synlett* **2005**, 2701–2719.
(2) Jackson, R. F. W.; Wishart, N.; Wood, A.; James, K.; Wythes, M. J. *J. Org. Chem.* **1992**, *57*, 3397–3404.
(3) Jackson, R. F. W.; Moore, R. J.; Dexter, C. S.; Elliot, J.; Mowbray, C. E. *J. Org. Chem.* **1998**, *63*, 7875–7884.
(4) Dexter, C. S.; Jackson, R. F. W.; Elliott, J. *J. Org. Chem.* **1999**, *64*, 7579–7585.

10.1021/jo801754k CCC: $40.75
Published on Web 10/15/2008

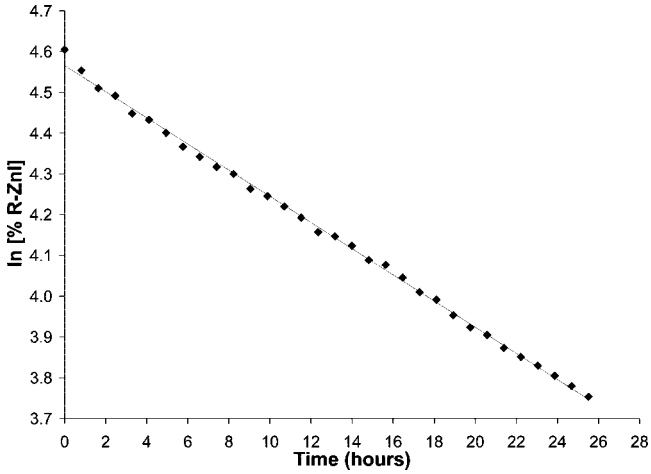

FIGURE 1. Kinetic analysis of the decomposition of organozinc reagent **2** in DMF-d_7 according to a first-order fit.

coupling reactions is influenced by the presence of functional groups within the zinc reagent. We have previously established that reagent **1** is the most stable of the three reagents[3] and have therefore concentrated on the behavior of reagents **2** and **3**.

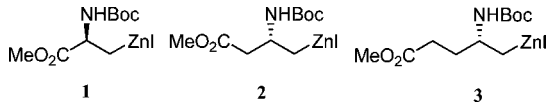

1 **2** **3**

Results and Discussion

We have previously studied the decomposition of the less stable reagent **2** using ^{1}H NMR spectroscopy, establishing that the main decomposition pathway is a unimolecular elimination reaction in both DMF-d_7 and THF-d_8. In our original kinetic work,[5] β-amino alkylzinc iodides were prepared from the corresponding alkyl iodides using zinc activated by prior treatment with 1,2-dibromoethane and chlorotrimethylsilane.[6] Recent preparative work has established that, at least in DMF, the use of 1,2-dibromoethane is unnecessary, and consequently, for all of the reactions reported in this paper, activation of zinc was carried out using chlorotrimethylsilane alone. This procedure, adapted from Hiemstra's protocol,[7] involves removal of the DMF (containing residual chlorotrimethylsilane and $ZnCl_2$) followed by drying of the activated zinc under vacuum and has the advantage that cheap undeuterated DMF can be used for the activation process. In order to establish the influence of this change in activation protocol on the elimination rate, the alkylzinc iodide **2** was prepared, and its elimination (at 291 K) was followed by ^{1}H NMR by measuring the integral of the methylene protons adjacent to zinc, relative to an internal standard (mesitylene). A small inflection was observed at the beginning of the first order plot (Figure 1), which was attributed to competing initial protonation of the alkylzinc iodide **2**, due to extraneous proton sources introduced during the transfer of the sample into the NMR tube. The first-order rate constant for the elimination reaction was determined to be 8.9×10^{-6} s^{-1}, following linear least-squares regression analysis. This contrasts with a value of 12.0×10^{-6} s^{-1} (at 291 K) for the same reagent prepared from zinc that had been activated with both 1,2-dibromoethane and chlorotrimethylsilane[5] (this value was calculated using the Arrhenius parameters determined in our earlier work,[5] since we had not made an experimental measurement of the rate constant at 291 K). This result suggests that the presence of halide ions can adversely influence the stability of β-amino alkylzinc iodides toward elimination. This finding is consistent with the improved results obtained for copper-promoted reactions of β-amino alkylzinc iodides when using catalytic amounts of CuBr·DMS,[8] rather than stoichiometric amounts of CuCN·2LiCl.[9]

SCHEME 1

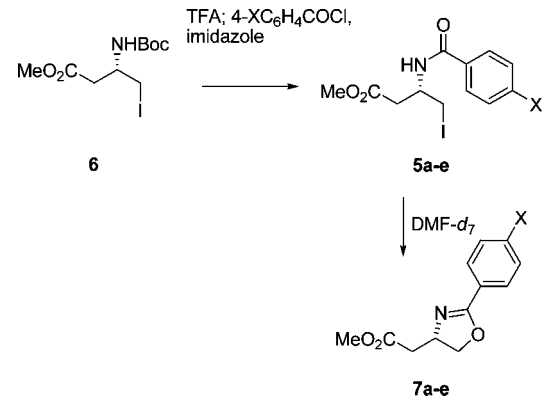

6 **5a-e** **7a-e**

Hammett Study of Benzamide Decomposition. In previous work,[5] the activation parameters for the first-order elimination of alkylzinc reagent **2** were determined in both THF and DMF. The negative entropy of activation was interpreted as indicating that a *syn*-elimination pathway is followed, in which coordination of the carbamate carbonyl group to zinc is required (eq 1). This coordination would be expected to have two consequences, namely increased electron density at zinc (thereby weakening the carbon−zinc bond) and enhancement of the leaving group ability of the carbamate, through Lewis acid activation.

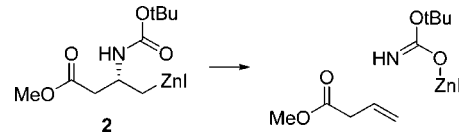

2 (1)

In order to probe further the mechanism of the elimination reaction, we undertook a study of the decomposition of a range of β-amino alkylzinc iodides **4a**−**e**, in which the amino group was protected as a para-substituted benzamide, since the results should be amenable to Hammett analysis. The alkyl iodides **5a**−**e**, precursors of the alkylzinc iodides **4a**−**e**, were prepared from the iodide **6** by Boc-deprotection and acylation. The overall yields for this process were poor due to rapid cyclization of the product iodides leading to the corresponding oxazolines **7a**−**e** (Scheme 1), but pure samples of all the iodides could be obtained. As expected, the more electron-rich substrates cyclized very readily, and in the case of the 4-methoxy derivative **5e**, cyclization was so rapid that a ^{1}H NMR spectrum (in DMF-d_7) obtained within 1 min of sample preparation showed approximately 50% of the oxazoline **7e**.

(5) Dexter, C. S.; Hunter, C.; Jackson, R. F. W.; Elliott, J. *J. Org. Chem.* **2000**, *65*, 7417–7421.
(6) Knochel, P.; Yeh, M. C. P.; Berk, S. C.; Talbert, J. *J. Org. Chem.* **1988**, *53*, 2390–2392.
(7) Karstens, W. F. J.; Stol, M.; Rutjes, F. P. J.; Hiemstra, H. *Synlett* **1998**, 1126–1128.
(8) Hunter, C.; Jackson, R. F. W.; Rami, H. K. *J. Chem. Soc., Perkin Trans. 1* **2001**, 1349–1352.
(9) Dunn, M. J.; Jackson, R. F. W.; Pietruszka, J.; Turner, D. *J. Org. Chem.* **1995**, *60*, 2210–2215.

TABLE 1. Preparation of Benzamides 5

benzamide	X	overall yield, %
5a	CN	23
5b	Br	25
5c	H	26
5d	CH_3	19
5e	CH_3O	18

Notwithstanding this instability, each of the iodides **5a**−**e** was efficiently converted into the corresponding zinc reagent **4a**−**e**, whose decomposition was then followed using ^{1}H NMR spectroscopy (eq 2). Rather surprisingly, no evidence for elimination was apparent in any example, but instead a simple protonation reaction occurred to give the products **8a**−**e**. In particular, the progress of protonation of the alkylzinc iodide **4b** (X = Br) was monitored up to 90% conversion (over 4 days) to allow differentiation between first- and second-order processes. Analysis of the data using linear least-squares regression analysis (Figure 2) clearly established that the protonation was first order, with a rate constant of 5.2×10^{-6} s^{-1}. (We are not aware of a previous determination of a rate constant for the protonation of a carbon−zinc bond.) The most credible interpretation of the small initial inflection in the plot is that this arises due to proton sources introduced during the transfer of the sample into the NMR tube. The decomposition of three other examples (**4a**, **4c**, and **4e**) to give the corresponding protonated products (**8a**, **8c**, and **8e**) was followed to around 35% conversion which, although insufficient to allow unambiguous determination of the reaction order, was enough to determine apparent first order rate constants, by analogy with reagent **4b**. In each case, the first-order rate constant was found to be very similar to that determined for **4b** and therefore essentially independent of the substituent X.

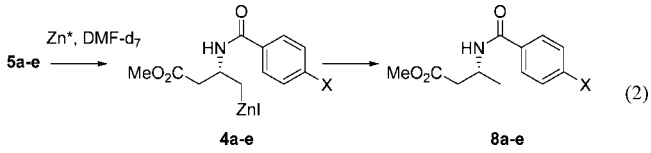

(2)

While this data is consistent with protonation by an external proton source present in substantial excess, this is unlikely given that the reactions were conducted in a sealed NMR tube. It therefore appears that the subsequent decomposition process

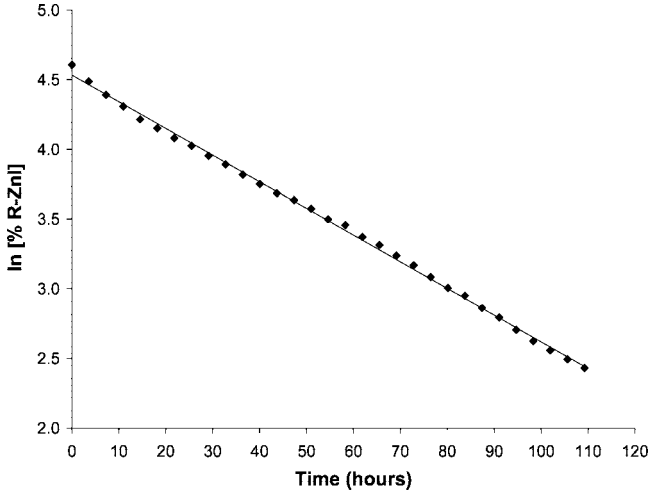

FIGURE 2. First-order plot for the (self-)protonation of reagent **4b** in DMF-d_7.

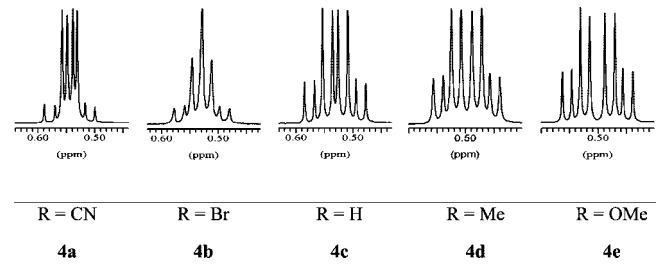

FIGURE 3. Appearance of CH_2ZnI in the ^{1}H NMR spectra of reagents **4a**−**e** in DMF-d_7.

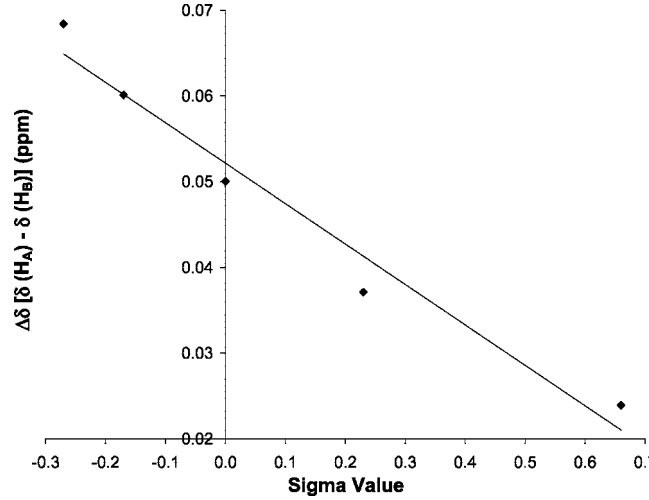

FIGURE 4. Plot of $\Delta\delta$ for the CH_2ZnI group in reagents **4a**−**e** against the Hammett parameter σ_x.

occurs by self-protonation. A possible mechanism involves tautomerisation of the amide in zinc reagent **4** into the enol form, so that intramolecular protonation of the carbon−zinc bond can occur (eq 3).

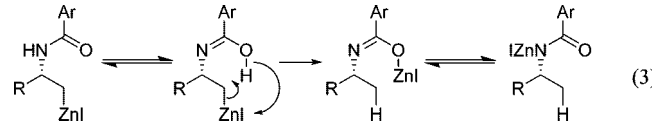

(3)

Although the benzamide study had not provided any insight into the elimination reaction of β-amino alkylzinc iodides, it had allowed the determination of the kinetics of a potentially competing protonation reaction. In addition, an interesting pattern was observed in the ^{1}H NMR spectra for the methylene group adjacent to zinc [CH_2ZnI] throughout the series of reagents **4a**−**e**, connecting the Hammett parameter of the aryl substituent, σ_x, to the difference in chemical shift of the two protons (Figure 3). A plot of $\Delta\delta$ (the difference in chemical shift between the signals for the two diastereoisotopic signals) against σ_x showed a significant correlation (Figure 4).

While the magnitude of the difference in chemical shift values ($\Delta\delta$) for diastereotopic protons is affected by numerous factors, including molecular conformation, temperature, and solvent, it is not generally possible to relate quantitatively the degree of nonequivalence to molecular structure.[10] However, in this case, it appears that the nature of the benzamide para substituent does influence the observed NMR spectra in a predictable way. The fact that $\Delta\delta$ is largest for the *p*-methoxy derivative is entirely

(10) Jennings, W. B. *Chem. Rev.* **1974**, *75*, 307–322.

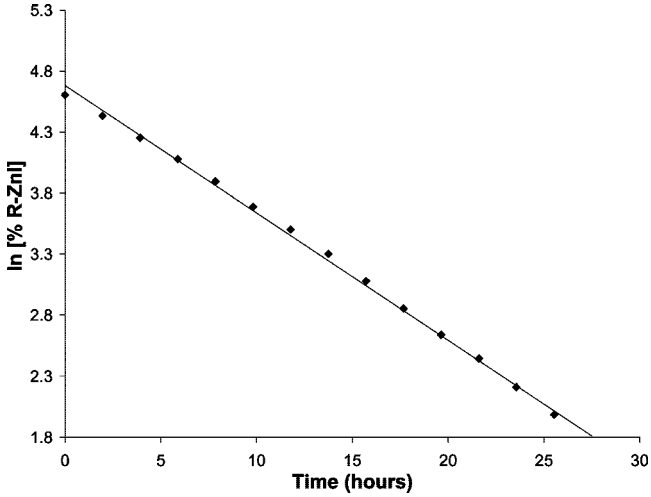

FIGURE 5. Kinetic analysis of the decomposition of organozinc reagent **3** in DMF-d_7 according to a first order fit.

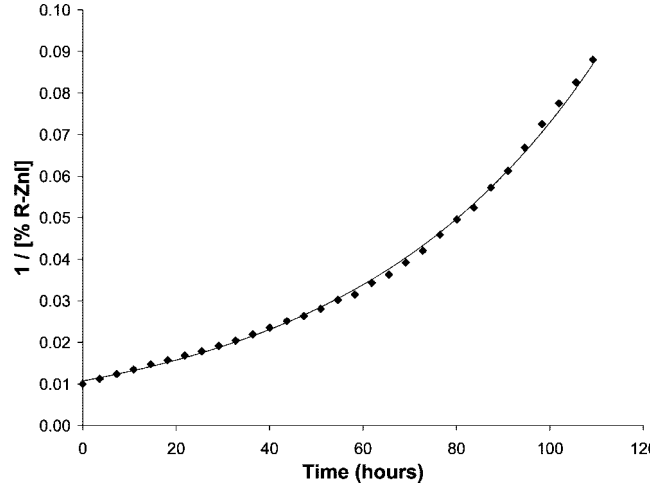

FIGURE 6. Kinetic analysis of the decomposition of organozinc reagent **3** in DMF-d_7 according to a second order fit.

consistent with the expected enhancement of coordination of the amidic carbonyl group to zinc, suggesting that this interaction is the principal determinant responsible for the observed pattern.

The fact that none of the zinc reagents **4a**−**e** showed evidence of decomposition via elimination demonstrates the substantial impact on stability of replacing the carbamate group in reagent **2** with a benzamide and suggested that rather subtle changes in the nitrogen protecting group might exert a profound influence on the behavior of β-amino alkylzinc iodides. Indeed, Knochel has previously reported that higher yields of coupling product are obtained using a simple β-benzamido alkylzinc iodide compared with those obtained from the corresponding acetamido-derivative.[11]

Study of the Decomposition of Organozinc Reagent 3. Attention now turned to the glutamic acid-derived alkylzinc iodide **3**, which was prepared in DMF-d_7, and its decomposition followed by ^{1}H NMR spectroscopy, as described above. The alkylzinc iodide **3** was found to decompose by 95% over the course of 24 h, substantially faster than reagent **2**, and it was therefore straightforward to compare a first- and second-order fitting in a rigorous manner. The first-order plot (Figure 5) shows that the decomposition was principally a first-order elimination reaction, leading to methyl 4-pentenoate **9**, although there was evidence for small amounts of the protonation product **10** (eq 4). The overall first-order decomposition rate constant, k, was determined by linear least-squares regression analysis to be 29×10^{-6} s^{-1}, substantially larger than the corresponding rate constant for the decomposition of reagent **2**. The second-order plot (Figure 6) clearly demonstrates the need to monitor the decomposition for more than one-half-life: approximately 50% of the zinc reagent had decomposed after 8 h, and both analyses produce a credible straight line plot over this time.

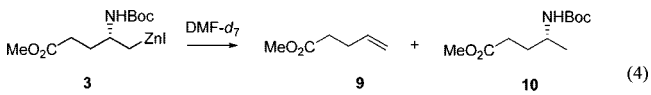

3 **9** **10** (4)

One limitation of this method of analysis is that the resulting decomposition rate also contains a component for the competing protonation of the zinc reagent and any other processes that result in a change in chemical shift of the methylene protons adjacent to zinc. This problem was overcome by the use of Specfit, a program developed for data collection and analysis in stopped-flow experiments using UV spectroscopy. By adapting the use of the program, it was possible to capture the values for the NMR integrals for the species present at each time point in the kinetic experiment. The initial concentration of each component was calculated from the ratio of the integrals and the initial concentration of the alkyl iodide. The change in concentration of each species over time was then measured (Figure 7), and the rate constant for each process, as well as the deviation from a calculated fit, was determined. The integrals were normalized to represent the same number of protons and the initial concentration of exogenous protons in the reaction medium was calculated from the integral of the protonated product at the end of the experiment.

Initially, a poor fit was observed between the experimental and calculated data using Specfit when the concentrations of zinc reagent, alkene byproduct, and protonated material were each taken into account. This primary analysis indicated a deficiency in the measured amounts of reagent **3** and the elimination product **9** toward the end of the experiment, compared to the calculated values (see the Supporting Information). This was attributed to the appreciable volatility of the elimination product, methyl 3-pentenoate **9** (bp 55−56 °C) which might be expected to diffuse into the headspace of the NMR tube where it would remain undetected. However, the ester **9** *was* detected by mass spectroscopy, and its odor was very evident in the NMR tube after completion of the experiment. An analysis of the kinetic data taking this into consideration, using only the concentration of zinc reagent **3** and protonation product **10**, resulted in theoretical and experimental data in very good agreement (Figure 8).

Analysis of the data for decomposition of **3** using Specfit showed that the rate constant for the elimination process was 24×10^{-6} s^{-1}. Given the overall first-order decomposition rate constant, k, of 29×10^{-6} s^{-1}, an upper limit of 5×10^{-6} s^{-1} can be defined for the rate constant for the corresponding protonation reaction to give **10**, very similar to that determined for protonation of the 4-bromobenzamide derivative **4b** (5.2×10^{-6} s^{-1}). Reanalysis of the data for the decomposition of reagent **2** using Specfit gave a first-order rate constant for the elimination of 9×10^{-6} s^{-1} (cf. 8.9×10^{-6} s^{-1}, the overall decomposition rate constant previously determined), showing that protonation of reagent **2** is not significant.

(11) Duddu, R.; Eckhardt, M.; Furlong, M.; Knoess, H. P.; Berger, S.; Knochel, P. *Tetrahedron* **1994**, *50*, 2415–2432.

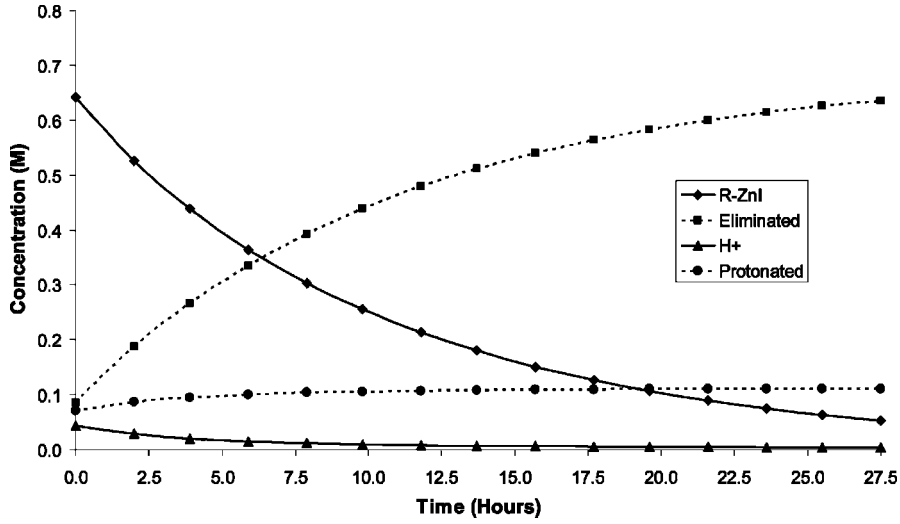

FIGURE 7. Kinetic analysis of the decomposition of organozinc reagent **3** in DMF-d_7 using Specfit.

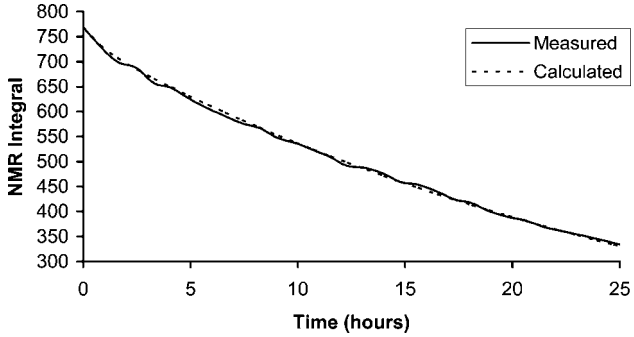

FIGURE 8. Plot of measured vs calculated values for the RCH_2ZnI integral, using the concentrations of zinc reagent **3** and protonated product **10**.

A likely explanation for the lower stability of glutamate−derived reagent **3** is reduced coordination by the ester carbonyl group to zinc in this compound, which results in the formation of a 7-membered ring **11**, compared to the lower homologue **2** derived from aspartic acid which would exist as a 6-membered ring **12**. Evidence for ester co-ordination has been provided through ^{13}C NMR studies[4] and is expected to compete with coordination by the Boc group to zinc, thereby reducing the rate of elimination to a greater extent in the case of reagent **2**.

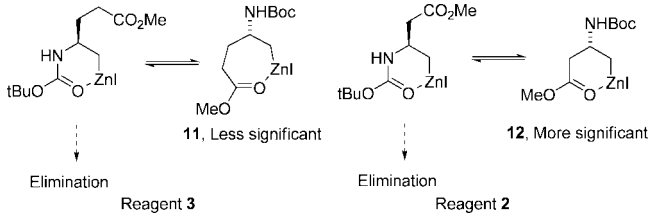

Stabilizing β-Amino Alkylzinc Iodides. Having established reliable methods for studying the decomposition of β-amino alkylzinc iodides, attention turned to evolving one or more strategies to inhibit these competing pathways so as to increase the yields of desired products in synthetic transformations. Our working hypothesis suggested that replacement of the carbamate group with one containing a less Lewis basic carbonyl group would result in reduced co-ordination and thereby depress the rate of elimination to provide more stable β-amino alkylzinc reagents. A comparative study of the decomposition of ana-

SCHEME 2. Synthesis of Iodides 21 and 22

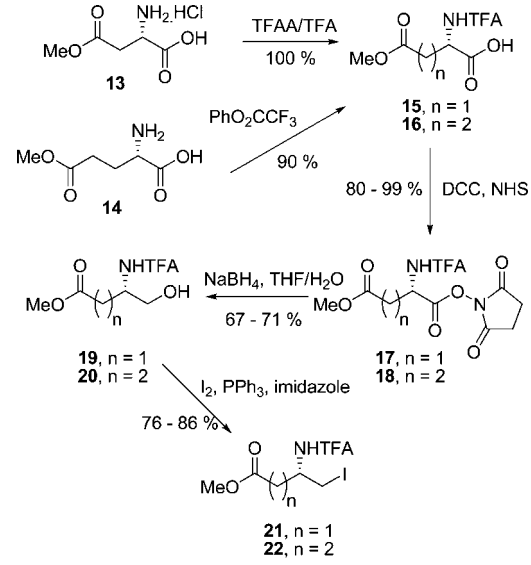

logues of the zinc reagents **2** and **3**, incorporating different *N*-protecting groups, was carried out according to the protocols already described. A preliminary account of a part of this work has appeared.[12]

A good candidate for the replacement of the *tert*-butoxycarbonyl group in compounds **2** and **3** was the trifluoroacetyl (TFA) group. As well as reducing, very substantially, the Lewis basicity of the carbonyl group, the amide proton should be much more acidic than that of a simple carbamate and offer an interesting test of the tolerance of organozinc iodides toward acidic protons. Accordingly, aspartic acid methyl ester hydrochloride **13**, and glutamic acid methyl ester **14** were each converted into the corresponding *N*-TFA derivatives, **15** and **16**, and the free carboxyl group was then reduced, via the *N*-hydroxysuccinimide esters, **17** and **18**, to give the corresponding alcohols **19** and **20**. Treatment of the alcohols **19** and **20** under standard iodinating conditions gave the precursor alkyl iodides **21** and **22** (Scheme 2).

Reaction of the iodide **21** with activated zinc in DMF-d_7 gave the corresponding organozinc reagent **23**. Interestingly, the

(12) Jackson, R. F. W.; Rilatt, I.; Murray, P. J. *Chem. Commun.* **2003**, 1242–1243.

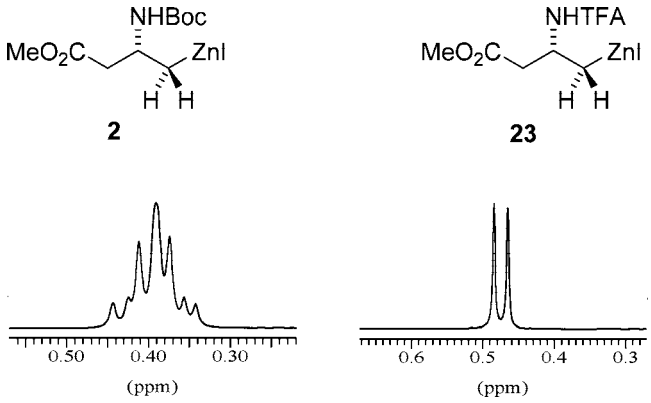

FIGURE 9. ^{1}H NMR signals for indicated protons of **2** and **23** in DMF-d_7. Reproduced with permission from The Royal Society of Chemistry.[12]

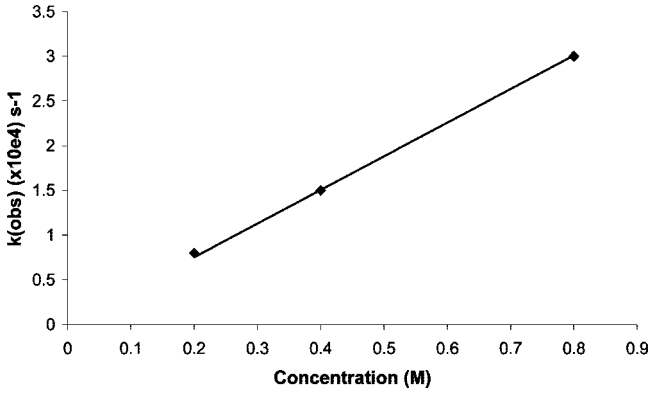

FIGURE 10. Plot of apparent first-order rate constants for the decomposition of reagent **23** against initial concentration, confirming that the decomposition is second order.

appearance of the signal (a simple doublet) for the two protons adjacent to zinc in the ^{1}H NMR spectrum of reagent **23** was radically different from that observed in reagent **2** (Figure 9).

More pertinently, the trifluoroacetamide **23** proved to be more stable toward β-elimination than the original reagent **2** (by a factor of more than 3-fold), as assessed by ^{1}H NMR spectroscopy. However, as a result of this enhanced stability, it became more challenging to monitor the decomposition over 2 half-lives due to the amount of instrument time required (zinc reagent **23** decayed by just 50% over 60 h). In our original interpretation of the data,[12] the elimination reaction was assumed to be a first-order process, by analogy with the corresponding Boc derivative. However, when the decomposition of reagent **23** was followed at a range of initial concentrations, the apparent first-order rate constants varied. A plot of these rate constants against concentration (Figure 10) gave a straight line, passing through the origin. Linear least-squares regression analysis indicated a second-order rate constant for the decomposition of reagent **23** of $3.8 \pm 0.5 \times 10^{-6}$ M^{-1} s^{-1}. Analysis of the data at each of these concentrations using Specfit indicated a second-order rate constant of $2.8 \pm 0.2 \times 10^{-6}$ M^{-1} s^{-1} for the elimination process, entirely consistent with the slightly larger overall decomposition rate constant.

The observation that introducing the TFA protecting group had not only reduced the rate of the elimination reaction but had also altered the mechanism of the process provided clear evidence of the pivotal role of the nitrogen protecting group in determining the properties of β-amino alkylzinc iodides. A possible explanation for the observed behavior is that, rather than the alkylzinc halide **23**, it is instead the corresponding dialkylzinc species **24**, (formed through fast Schlenk pre-equilibrium), which undergoes the elimination reaction (eq 5). Although the NMR spectra are consistent with the major solution species being the alkylzinc iodide, the equilibrium concentration of the dialkylzinc species **24** is related to the square of the concentration of the alkylzinc iodide **23**, explaining the observed second-order dependence. The observed change in mechanism probably arises from the reduced ability of the carbonyl oxygen of the trifluoroacetamide group to coordinate to zinc (cf. the NMR evidence in Figure 9) and therefore to promote the *syn*-elimination believed to occur in the case of the corresponding Boc derivative **2**. The alternative elimination pathway for a β-amino alkylzinc iodide, namely *anti*-elimination, is less likely to occur due to the electron-withdrawing character of the iodide ligand (which in turn reduces the electron density at the carbon atom bound to zinc). However, the dialkylzinc species **24**, lacking the influence of the iodide ligand, is better able to undergo *anti*-elimination. Whatever the reason, the second-order nature of the elimination process for **23** means that higher reagent concentrations lead to faster decomposition. This stands in marked contrast to the analogous Boc derivative **2**, where high concentrations are optimal to promote the bimolecular processes involved in bond-forming reactions.

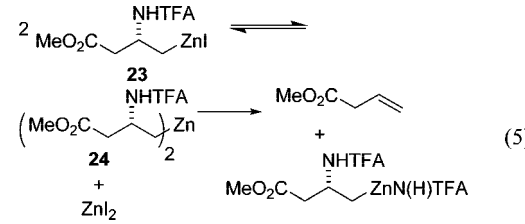

(5)

The rate of decomposition of the glutamic acid-derived alkylzinc reagent **25** was then investigated, and as expected, this compound decomposed to give methyl 4-pentenoate **9**, albeit rather slowly. The extent of decomposition of **25** was, therefore, insufficient to assign an order to the elimination reaction rigorously, but it is reasonable to assume, by analogy with the elimination of reagent **23**, that a second-order reaction takes place. The (assumed) second-order rate constant (determined using Specfit) for the elimination of the glutamic acid-derived alkylzinc reagent **25** was $3.3 \pm 0.5 \times 10^{-6}$ M^{-1} s^{-1}, very similar to that observed for the lower homologue **23**. Replacement of the Boc group in compound **3** by the TFA group had resulted therefore, as predicted, in a reagent, **25**, which was substantially more stable toward elimination.

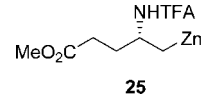

Comparison of the ^{13}C NMR spectra of the *N*-TFA-protected zinc reagents with their *N*-Boc counterparts revealed that the carbonyl oxygen−zinc interaction had been suppressed (Table 2). Interestingly, no significant differences in ester coordination, as revealed by the measurement of the $\Delta\delta$ values for the ester and amide/carbamate carbonyl groups, were observed for each pair of zinc reagents.

Reactivity of Organozinc Reagents in Negishi Cross-Coupling. Having established the influence of the nitrogen protecting group on stability, the next goal was to understand

TABLE 2. Changes in ^{13}C NMR Chemical Shift of Carbonyl Groups upon Zinc Insertion in DMF-d_7 for Zinc Reagents 2, 23, 3, and 25

	$\Delta\delta$ C=O ($\delta_{(R\text{-}ZnI)} - \delta_{(R\text{-}I)}$)			
	2	**23**	**3**	**25**
N-protecting group	−0.5	−1.9	−0.7	−1.8
ester	+0.9	+1.0	+0.1	+0.5

how this change affected the reactivity of β-amino alkylzinc iodides in Negishi cross-coupling reactions. It has been established that the rate-limiting step in the Negishi reaction is the transmetalation step, in which the organic group is transferred from zinc to palladium.[13] While the second-order rate constant for the stoichiometric reaction between $(Ph_3P)_2Pd(I)Ph$ and (*E*)-1-octenylzinc chloride to give (*E*)-1-octenylbenzene has been determined ($2.9\ M^{-1}\ min^{-1} = 4.83\ 10^{-2}\ M^{-1}\ s^{-1}$),[13] there is rather little experimental rate data for Negishi cross-coupling reactions conducted under catalytic conditions.[14] We were pleased to discover that NMR spectroscopy, in combination with data analysis using Specfit, allowed the measurement of pseudo-second-order constants, *k*, for the cross-coupling reaction of the four reagents **2**, **3**, **23**, and **25** with iodobenzene, catalyzed by $Pd_2(dba)_3$ and P(*o*-tol)$_3$ (eq 6), according to the rate law in eq 7, at particular concentrations of palladium and phosphine ligand.

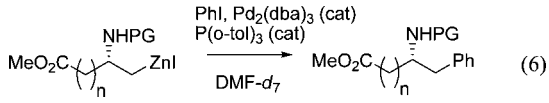

(6)

$$\text{rate} = k[\text{RZnI}][\text{PhI}] \quad (7)$$

In contrast to the kinetic analysis of the elimination reaction, a significant technical challenge was the short time frame within which the Negishi reactions of some of the reagents went to completion. When typical catalyst loadings were used [2.5 mol % of $Pd_2(dba)_3$ and 10 mol % of P(*o*-tol)$_3$], the cross-coupling reactions were essentially complete by the time the first NMR spectrum was recorded. This obstacle was straightforwardly overcome by reducing the catalyst loading[15] by a factor of 6 [to 0.42 mol % of $Pd_2(dba)_3$ and 1.67 mol % of P(*o*-tol)$_3$].

Using Specfit, we observed a good correlation between the experimental and theoretical values of the integrals of the diagnostic signals in the ^1H NMR spectra (specifically the benzylic protons in the product), although a slight increase in reaction rate toward the end of the experiment was observed (Figure 11). The deviation in reaction rate over the course of the reaction may be due to a number of factors, including the change in concentration of ZnI_2 affecting the Schlenk equilibrium[16] and catalyst/ligand equilibria or matrix effects, in turn due to the relatively high concentrations at which the reactions were conducted.

Pseudo-second-order rate constants for the Negishi cross coupling of reagents **2**, **3**, **23**, and **25** with iodobenzene, according to eq 7, are given in Table 3, together with yields of isolated products from the NMR experiment. These yields are obtained from reactions conducted under suboptimal conditions

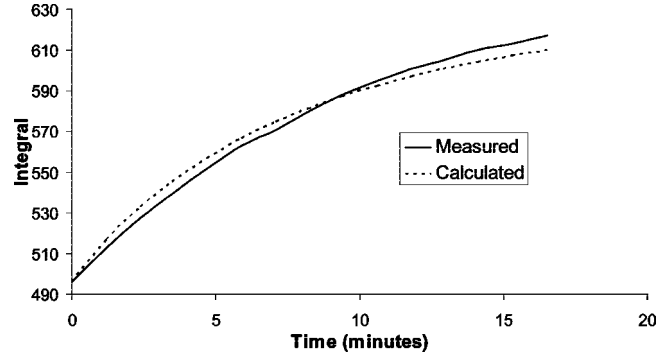

FIGURE 11. Plot of measured versus calculated values for the product integral of the reaction of reagent **23** with PhI.

TABLE 3. Comparison of Elimination Rate Constants, Reaction Rate Constants, and Isolated Yield from Negishi Cross-Coupling with Iodobenzene

organozinc reagent	N-protecting group	elimination rate constant ($\times 10^{-6}\ s^{-1}$ or $\times 10^{-6}\ M^{-1}\ s^{-1}$)	reaction rate constant[a] ($\times 10^{-4}\ M^{-1}\ s^{-1}$)	isolated yield[b] (%)
2	Boc	9.0	0.6	51
23	TFA	2.8	0.6	55
3	Boc	24.0	4.3	59
25	TFA	3.3	7.5	79

[a] Pseudo-second-order rate constant determined at 291 K using 0.42 mol % $Pd_2(dba)_3$ and 1.67 mol % P(*o*-tol)$_3$ as catalyst. [b] All yields are based on starting alkyl iodide.

(in an NMR tube), and represent a lower limit to the efficiency of the process (vide infra). Also included for reference are the rate constants determined for the elimination reactions. It is noteworthy that the rate constants for the catalytic cross-coupling of zinc reagents **2**, **3**, **23**, and **25** with iodobenzene are similar in magnitude to the rate constant for the stoichiometric reaction between $(Ph_3P)_2Pd(I)Ph$ and (*E*)-1-octenylzinc chloride (vide supra), when the amount of palladium catalyst (0.84 mol %) is taken into account ($4.83\ 10^{-2}\ M^{-1}\ s^{-1} \times 8.4\ 10^{-3} = 4.1\ 10^{-4}\ M^{-1}\ s^{-1}$). This provides circumstantial evidence that, at least for the catalytic cross-coupling reactions included in the present study, it is the transmetalation step that is rate-limiting, and the main factor determining the efficiency of the cross-coupling procedure, rather than the stability of the reagent. Nonetheless, it is interesting that the lower stability, but higher reactivity, of reagent **3** results in a similar isolated yield to that obtained with reagent **23**. It appears that the rate of the cross-coupling reaction is primarily dependent upon the proximity of the ester group, rather than the nature of nitrogen protecting group, since both glutamic acid derived reagents **3** and **25** are substantially more reactive than the aspartic acid derivatives **2** and **23**.

Preparative Negishi Cross-Coupling Reactions. When preparative Negishi cross-coupling reactions of reagent **23** were carried out with aryl iodides, the isolated yields of the products **26** were consistent, and also broadly similar to those previously obtained with reagent **2** (Scheme 3, Table 4). In the case of 4-iodonitrobenzene, no product was obtained under standard conditions, probably due to competing reduction of the nitro group with metallic zinc. To avoid this, the solution of the reagent **23** was transferred via syringe to a separate flask, leaving behind excess zinc, and reacted with the electrophile under standard conditions to furnish the product in 65% yield. This leads to the conclusion that, while reagent **23** is more stable toward β-elimination than reagent **2**, its overall efficiency in

(13) Negishi, E.; Takahashi, T.; Baba, S.; Vanhorn, D. E.; Okukado, N. *J. Am. Chem. Soc.* **1987**, *109*, 2393–2401.
(14) Casares, J. A.; Espinet, P.; Fuentes, B.; Salas, G. *J. Am. Chem. Soc.* **2007**, *129*, 3508–3509.
(15) Huang, Z.; Qian, M.; Babinski, D. J.; Negishi, E.-i. *Organometallics* **2005**, *24*, 475–478.
(16) Denmark, S. E.; O'Connor, S. P. *J. Org. Chem.* **1997**, *62*, 3390–3401.

SCHEME 3. Preparation of β-Amino Acids 26 by Negishi Cross-Coupling

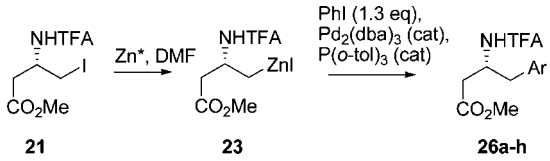

21 23 26a-h

TABLE 4. Negishi Cross-Coupling of Reagent 23 with Aryl Iodides

aryl iodide	product	Ar	yield[a] (%)
4-MeC$_6$H$_4$I	**26a**	4-Me-C$_6$H$_4$	64 (73)[b]
4-MeOC$_6$H$_4$I	**26b**	4-MeOC$_6$H$_4$	69 (68)[b]
4-O$_2$NC$_6$H$_4$I	**26c**	4-O$_2$NC$_6$H$_4$	65 (89)[b]
PhI	**26d**	Ph	72 (73)[b]
4-NCC$_6$H$_4$I	**26e**	4-NCC$_6$H$_4$	77 (−)
1-NaphthylI	**26f**	1-naphthyl	70 (61)[b]
4-BrC$_6$H$_4$I	**26g**	4-BrC$_6$H$_4$	53 (58)[b]
4-FC$_6$H$_4$I	**26h**	4-FC$_6$H$_4$	74 (65)[b]

[a] All yields are based on the starting alkyl iodide **21**. [b] Yields in parentheses of the corresponding Boc-derivative obtained using reagent **2** and reported previously.[4]

SCHEME 4

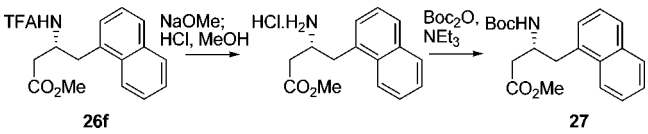

26f 27

cross-coupling reactions, the key parameter, is similar. Nonetheless, reagent **23** does allow access to β^3-amino acids **26** containing a base-labile nitrogen protecting group, and so may offer practical advantages of orthogonality in synthetic applications.

In order to demonstrate that the no racemisation had occurred during the Negishi reaction, the naphthyl derivative **26f** was converted into the previously reported *N*-Boc derivative **27** (93% overall)[4] by treatment with NaOMe in MeOH, followed by isolation of the hydrochloride salt, and standard Boc protection (Scheme 4). Measurement of the optical rotation and comparison with the literature value[4] revealed that no detectable racemization had occurred.

As established in the present study, replacement of the Boc-group in reagent **3** with a trifluoroacetyl group in reagent **25** results in an intermediate that is not only more stable with respect to elimination but also slightly more reactive in the Negishi cross-coupling. This combination ensured that excellent yields of γ-amino acids **28** were obtained in preparative cross-coupling of reagent **25** with a range of aryl iodides (Table 5, Scheme 5). The increase in yield when using reagent **25** compared to **3** for the coupling with 2-fluoroiodobenzene, a normally inefficient substrate in such processes, is significant. Of the β-amino alkylzinc iodides prepared to date, reagent **25** is likely to display the least significant intramolecular coordination of zinc by the carbonyl group of either the ester (formation of a 7-membered ring, cf. **11**) or the trifluoroacetamide, thereby diminishing the two factors which suppress the reactivity of the reagent.

Influence of the Carboxylic Acid on the Stability and Reactivity of β-Amino Alkylzinc Iodides. Having established the substantial influence that the nitrogen-protecting group can have on the behavior of β-amino alkylzinc iodides derived from aspartic and glutamic acid, attention was focused on the effect

SCHEME 5. Preparation of γ-Amino Acids 28 by Negishi Cross-Coupling

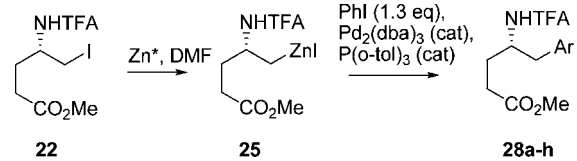

22 25 28a-h

TABLE 5. Negishi Cross-Coupling of Reagent 25 with Aryl Iodides

aryl iodide	product	Ar	yield,[a] %
4-MeC$_6$H$_4$I	**28a**	4-MeC$_6$H$_4$	79 (68)[b]
4-MeOC$_6$H$_4$I	**28b**	4-MeOC$_6$H$_4$	79 (68)[b]
PhI	**28c**	Ph	88 (68)[b]
2-H$_2$NC$_6$H$_4$I	**28d**	2-H$_2$NC$_6$H$_4$	62 (56)[b]
2-FC$_6$H$_4$I	**28e**	2-FC$_6$H$_4$	51 (34)[b]

[a] All yields are based on the starting alkyl iodide **22**. [b] Yields in parentheses obtained using reagent **3** and reported previously.[4]

SCHEME 6. Preparation of *N*-Boc-Protected Weinreb Amide 33

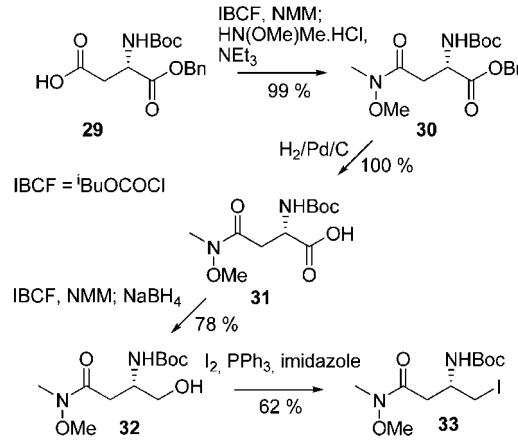

exerted by the carboxylic acid function. The initial hypothesis was that replacement of the ester with an alternative functional group able to coordinate zinc more strongly might provide reagents stabilized toward elimination, especially in cases where carbamate coordination had been implicated in this decomposition pathway. In the case of the trifluoroacetyl reagents, the outcome was less obviously predictable, since elimination did not appear to proceed by coordination of the nitrogen protecting group to zinc. The group selected to replace the ester was the Weinreb amide,[17] given its well-established pedigree as a metal coordinating group,[18,19] as well as its value for further synthetic manipulation.

Synthesis of the required *N*-Boc-protected Weinreb amide **33** started from commercially available *N*-Boc aspartic acid α-benzyl ester **29** (Scheme 6). Weinreb amide **30** was formed in quantitative yield by reaction with *N*,*O*-dimethylhydroxylamine hydrochloride, according to the literature procedure.[20] The benzyl ester was cleaved by hydrogenation and the resulting acid **31** was reduced to alcohol **32** via sodium borohydride reduction of a mixed anhydride and converted into the iodide **33** under standard conditions.

(17) Nahm, S.; Weinreb, S. M. *Tetrahedron Lett.* **1981**, *22*, 3815–3818.
(18) Sibi, M. P. *Org. Prep. Proced. Int.* **1993**, *25*, 15–40.
(19) Singh, J.; Satyamurthi, N.; Aidhen, I. S. *J. Prakt. Chem.* **2000**, *342*, 340–347.
(20) Adlington, R. M.; Baldwin, J. E.; Catterick, D.; Pritchard, G. J. *J. Chem. Soc., Perkin Trans. 1* **1999**, 855–866.

SCHEME 7

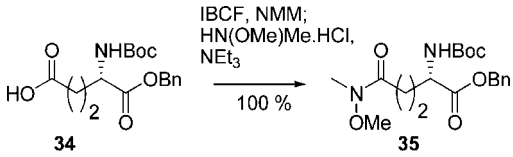

SCHEME 8. Preparation of Iodides 44 and 45

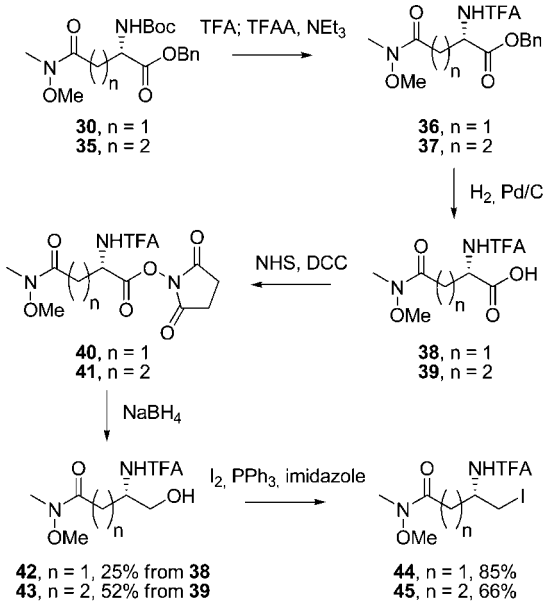

The synthesis of the *N*-TFA-protected, aspartic acid-derived Weinreb amide used a similar protocol, starting from the Boc-protected Weinreb amide **30**. The analogous glutamic acid derived Weinreb amide derivative **35** was synthesized from commercially available protected glutamic acid **34** (Scheme 7) using the same procedure employed for the preparation of **30**.

Benzyl esters **30** and **35** were converted into the TFA derivatives **36** and **37**, respectively, which were then transformed into the carboxylic acids **38** and **39** in quantitative yield by hydrogenation (Scheme 8). Although problems were encountered upon attempted reduction of the carboxylic acids **38** and **39** using the mixed anhydride protocol used previously, reduction via the *N*-hydroxy succinimide esters was achieved. However, in the case of the aspartic acid derivative, reduction to the alcohol **42** proceeded in low yield (25%) due to loss of the trifluoroacetyl group under the reaction conditions. Although such deprotections are known, more forcing conditions (reflux) are normally required.[21] Reduction of the glutamic acid homologue proceeded more efficiently to give alcohol **43** in an unoptimised yield of 52% over two steps. Iodination of alcohols **42** and **43** proceeded smoothly to give the desired iodides **44** and **45**.

The alcohol **42** was subsequently synthesized more efficiently via a protecting group transformation of the Boc-protected β amino alcohol **32**, involving deprotection/reprotection in excess of trifluoroacetic anhydride (Scheme 9).

The precursor iodides **33**, **44**, and **45**, were transformed into the zinc reagents **46**−**48** and a comparison made of their ^{13}C NMR spectra. Evidence for a significant interaction between the Weinreb amide and zinc was provided by a shift in the ^{13}C signal due to the amide carbonyl group for both aspartic acid

SCHEME 9

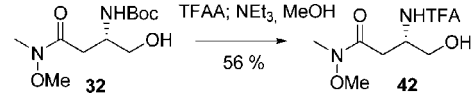

TABLE 6. Changes in ^{13}C-NMR Chemical Shift of Carbonyl Groups upon Zinc Reagent Formation in DMF-d_7 for Weinreb amides

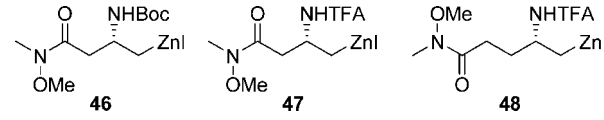

	$\Delta\delta$ C=O ($\delta_{(R\text{-}ZnI)} - \delta_{(R\text{-}I)}$)		
	46	**47**	**48**
N-protecting group	−0.3	−1.8	−1.9
Weinreb amide	+2.9	+2.5	+0.7

derivatives **46** and **47** but not for the glutamic acid homologue **48** (Table 6). In this system, it is hard to exclude the possibility that such a shift may also be due to a hydrogen-bonding interaction between the Weinreb amide and the NH residue. The shifts in the Boc[4] and TFA (this work) carbonyl carbon signals upon zinc insertion were typical of those already observed.

Contrary to our expectations, all three zinc reagents **46**, **47**, and **48** proved to decompose more quickly than the corresponding methyl ester analogues, and it was therefore possible in each case to follow the elimination reaction to 90% completion, allowing a definitive assessment of the order of the elimination reaction. The Boc Weinreb amide derivative **46** decomposed by a first-order process as expected, albeit with a rate constant of 62.5×10^{-6} s^{-1}, some 7 times larger than the elimination rate constant for the corresponding methyl ester **2**. However, it was surprising that both trifluoroacetyl derivatives **47** and **48** also decomposed via first order processes, with rate constants of 8.1×10^{-6} s^{-1} and 10.4×10^{-6} s^{-1}, respectively.

Direct comparison of the first-order rate constants for decomposition of reagents **46** and **47** shows unambiguously that the trifluoroacetamido reagent **47** is substantially more stable than the Boc-derivative **46**. This result, for two reagents that are directly comparable, demonstrates clearly that the key parameter in promoting elimination of β-amino alkylzinc iodides, by a first-order process, is the Lewis basicity of the nitrogen protecting group and not its intrinsic leaving group ability.

There are two possible rationalizations for the decrease in stability of the zinc reagents containing a Weinreb amide. In principle, the elimination can occur from either of two conformations. In pathway A, a hydrogen bond between the acidic trifluoroacetamide proton and the Weinreb amide (observed in a related system[22]) organizes the system in a conformation disposed toward *syn*-elimination, despite the poor Lewis basicity of the trifluoroacetyl group. In pathway B, the strongly coordinating Weinreb amide might increase the electron density on zinc sufficiently to allow a normal *anti*-elimination to take place (Scheme 10). Although the ^{13}C NMR evidence suggests that the trifluoroacetyl group does not coordinate to zinc, the reactive conformation may, of course, not be the major solution structure, so it is not possible to exclude pathway A on this basis alone.

(21) Weygand, F.; Frauendorfer, E. *Chem. Ber.* **1970**, *103*, 2437–2449.

(22) Hanessian, S.; Yang, H.; Schaum, R. *J. Am. Chem. Soc.* **1996**, *118*, 2507–2508.

SCHEME 10. Possible Mechanisms for the First-Order Elimination of Weinreb Amide Containing β-Amino Alkylzinc Iodides

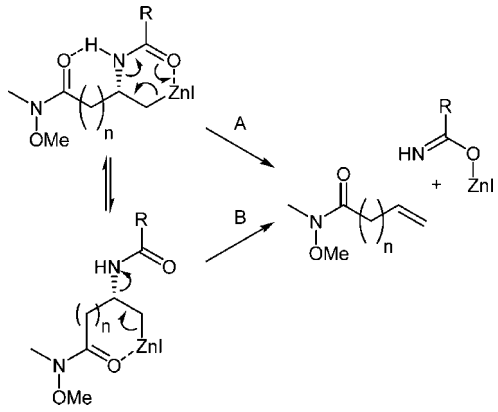

SCHEME 11. Cross-Coupling of Zinc Reagents 47 and 48

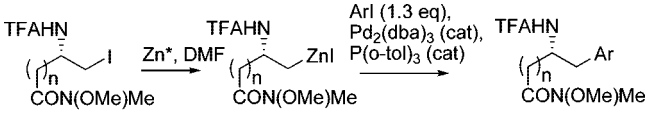

44, n = 1
45, n = 2

47, n = 1
48, n = 2

49, n = 1
50, n = 2

TABLE 7. Isolated Yields from the Negishi Cross-Coupling of Zinc Reagents 47 and 48 with Substituted Aryl Iodides

aryl Iodide	zinc reagent	product	Ar	yield,[a] %
4-MeC_6H_4I	**47**	**49a**	4-MeC_6H_4	68
4-$MeOC_6H_4I$	**47**	**49b**	4-$MeOC_6H_4$	59
PhI	**47**	**49c**	Ph	56
4-NCC_6H_4I	**47**	**49d**	4-NCC_6H_4	67
1-naphthylI	**47**	**49e**	1-naphthyl	60
4-BrC_6H_4I	**47**	**49f**	4-BrC_6H_4	53
4-MeC_6H_4I	**48**	**50a**	4-MeC_6H_4	70
4-$MeOC_6H_4I$	**48**	**50b**	4-$MeOC_6H_4$	69
PhI	**48**	**50c**	Ph	77
2-$H_2NC_6H_4I$	**48**	**50g**	2-$H_2NC_6H_4$	51
2-FC_6H_4I	**48**	**50h**	2-FC_6H_4	46

[a] All yields are based on the starting alkyl iodide **44** or **45**.

Notwithstanding the greater instability of the Weinreb amide trifluoroacetamide organozinc reagents **47** and **48**, Negishi cross-coupling with a range of substituted iodobenzenes (Scheme 11) gave the expected products **49** and **50** in moderate but generally consistent yields (Table 7, Scheme 11). Preparative cross-coupling of the *N*-Boc protected Weinreb amide **46** was not carried out due to its substantially greater instability with respect to elimination.

Finally, encouraged by a report on the addition of organometallic reagents to *N*-sulfinyl β-amino Weinreb amides,[23] we investigated the addition of organometallic reagents to a typical Weinreb amide cross coupling product, **49e**. This intermediate was treated with representative Grignard reagents and one organolithium reagent, giving substitution products **51a**−**d** in good to excellent yield (Scheme 12). Thus, reagent **47** functions as the synthetic equivalent of the chiral aminoketone synthon **52**, illustrating the potential of this method for the synthesis of β-amino ketones.

Attempted reaction of the Weinreb amide **49e** with isopropylmagnesium chloride gave *N*-methyl amide **53** in 95% yield.

(23) Davis, F. A.; Prasad, K. R.; Nolt, M. B.; Wu, Y. Z. *Org. Lett.* **2003**, *5*, 925–927.

SCHEME 12. Addition of Organometallic Reagents to Weinreb Amide 49e

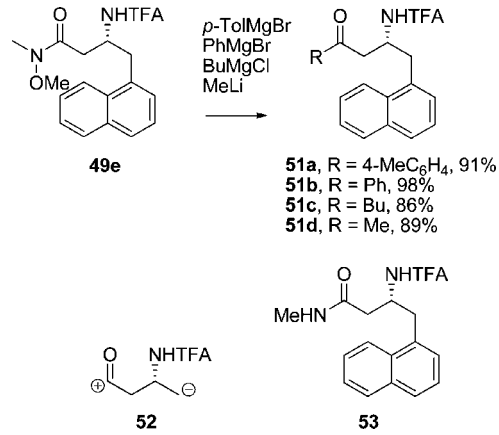

49e

51a, R = 4-MeC_6H_4, 91%
51b, R = Ph, 98%
51c, R = Bu, 86%
51d, R = Me, 89%

52

53

In this case, the Grignard reagent acted as a base, promoting decomposition of the Weinreb amide via elimination of the methoxy group. This mode of reactivity of Weinreb amides has been reported.[24]

Conclusions. The counter-intuitive hypothesis that the rate of elimination of β-amino alkylzinc iodides can be reduced by introducing a more electron-withdrawing nitrogen protecting group has been validated. Furthermore, the observation that replacement of a Boc group with a TFA group changes the mechanism of the elimination reaction provides direct evidence that the interaction of the carbonyl group with zinc is pivotal in the elimination process. Kinetic analysis of the Negishi cross-coupling of iodobenzene with β-amino alkylzinc iodides, derived from aspartic and glutamic acids, has shown that the nature of the nitrogen protecting group has only a marginal effect on the overall rate, and that the main factor that determines reactivity is the proximity of the ester group. From a synthetic point of view, the results suggest that the TFA group is an excellent choice for protection of nitrogen in β-amino alkylzinc iodides, since the precursor iodides are stable with respect to oxazoline formation, without adversely affecting the stability or reactivity of the alkylzinc iodide.

Experimental Section

General Procedure A: Preparation of Zinc Reagents for Kinetic NMR Experiments in DMF-d_7. Zinc dust (0.236 g, 3.6 mmol, 6.0 equiv) was added to a 25 mL round-bottom flask, with sidearm, containing a rugby ball-shaped stirrer bar. The flask was flushed with nitrogen and DMF (nondeuterated, 0.75 mL) and TMSCl (50 μL) were added under nitrogen via syringe. The solution was observed to effervesce and the mixture was stirred at room temperature for 5 min, at the fastest speed possible. The zinc was allowed to settle and the supernatant solution was removed via syringe, followed by drying of the zinc under vacuum using heating from a hot air gun. When the flask had cooled, the iodide (0.6 mmol, 1.0 equiv) was added as a solid and the flask flushed again with nitrogen, followed by the addition of DMF-d_7 (0.75 mL) via syringe. Note: If the iodide is a liquid it is dissolved in DMF-d_7 (0.75 mL) and added to the zinc via syringe. The solution was stirred at the fastest speed and cooling using a cold water bath was applied at the onset of an exotherm, which is usually a reliable indication that the zinc insertion has occurred. Note: If the insertion is slow, an exotherm may not be observed and the insertion can be followed by TLC (Et_2O). Mesitylene (25 μL, 0.3 mmol) was added, the zinc

(24) Graham, S. L.; Scholz, T. H. *Tetrahedron Lett.* **1990**, *31*, 6269–6272.

was allowed to settle and the supernatant transferred via syringe to a nitrogen-filled NMR tube fitted with a Young's tap. Reference used for DMF-d_7 (δ_H 2.74, δ_C 162.70).

General Procedure B: Preparation of Zinc Reagents and Monitoring of Cross-Coupling Reaction by NMR Spectroscopy in DMF-d_7. General procedure A is followed until completion of the zinc insertion. At this point, mesitylene (25 μL), the electrophile (0.78 mmol, 1.3 equiv), and finely ground P(*o*-tol)$_3$ and $Pd_2(dba)_3$ were added, and the solution was stirred for 1 min. Note: the P(*o*-tol)$_3$ was ground in a vial using a spatula before weighing. This aids dissolution. The zinc was allowed to settle and the supernatant transferred via syringe to a nitrogen-filled NMR tube fitted with a Young's tap. At the completion of the reaction, the mixture was worked up using procedure C.

General Procedure C: Palladium-Catalyzed Cross-Coupling of Electrophiles with Organozinc Reagents. Alkyl iodide (0.6 mmol, 1.0 equiv) was weighed into a vial and placed under high vacuum during the Zn activation period. A 25 mL round-bottom flask with sidearm, containing a rugby ball-shaped stirrer bar was removed from the oven and zinc dust added (0.236 g, 3.6 mmol, 6.0 equiv). The flask was flushed with nitrogen and dry DMF (0.75 mL) and TMSCl (100 μL, 0.8 mmol) were added under nitrogen via syringe. The solution was observed to effervesce and the mixture was stirred at room temperature for 5 min, at the fastest speed (note: the DMF occasionally changes to a yellow color during this period). The zinc was allowed to settle and the supernatant solution was removed via syringe, followed by drying of the zinc under vacuum using heating from a hot air gun. The iodide was dissolved in DMF (0.75 mL) under nitrogen and transferred to the zinc via syringe. The solution was stirred at 0 °C and the insertion judged by TLC (dichloromethane) to be complete within 5 min. Tris(dibenzylideneacetone)dipalladium (17.9 mg, 0.02 mmol, 2.5 mol % cf. electrophile), tri-*o*-tolylphosphine (23.8 mg, 0.08 mmol, 2 equiv relative to Pd), and the electrophile (1.3 equiv relative to the iodide) were added to the flask. The flask was covered in aluminum foil and stirred overnight. The DMF was evaporated under reduced pressure and the crude oil dissolved in CH_2Cl_2 (5 mL) and partitioned between diethyl ether (60 mL) and water (20 mL). The organic phase was washed with brine (10 mL), dried ($MgSO_4$), filtered, and evaporated under reduced pressure to give the crude product.

General Procedure D: Iodination of Alcohols. Iodine, triphenylphosphine, and imidazole were added to dry CH_2Cl_2 under nitrogen with stirring (caution: exothermic!). A white precipitate formed, and the solution turned dark orange. A solution of the alcohol in the minimum volume of dry CH_2Cl_2 was added slowly via syringe, whereupon the solution became lighter orange. The reaction was usually observed to have gone to completion at this point and can be checked by TLC. The mixture was filtered, the filtrate concentrated under reduced pressure, and the residue dissolved in Et_2O. The insoluble material was removed by filtration, and the filtrate washed with saturated sodium thiosulfate solution (50 mL), whereupon the orange color disappeared. The organic phase was washed with brine (20 mL), dried over $MgSO_4$, and filtered and the solvent evaporated under reduced pressure to give the crude product.

Acknowledgment. We thank OSI Pharmaceuticals for support of a Ph.D. studentship (I.R.), the RSC for a Journals Grants, Dr. B. Taylor and Miss S. Bradshaw for NMR spectra, Drs. N. Buurma and N. H. Williams for advice on analysis of the kinetic data, and Dr. P. J. Murray for continued interest in the project and for very helpful comments on the manuscript.

Supporting Information Available: General experimental procedures, including procedures for analysis of kinetic data; experimental procedures and characterization data for all compounds; ^1H and ^{13}C NMR spectra for all isolated compounds. This material is available free of charge via the Internet at http://pubs.acs.org.

JO801754K